International Academic Institute for Science and Technology

International Academic Journal of Science and Engineering
Vol. 3, No. 2, 2016, pp. 176-187.

ISSN 2454-3896

International Academic Journal of Science and Engineering

www.iaiest.com

Development of Feature Adaptation Models for Proper Registration of Aerial Images

Seyyed Naser Kazemi[a], Hossein Sohooli Zadeh[b]
a. Computer Science, Islamic Azad University, Ashtian Branch
b.Advisor Professor

Abstract

Unmanned aerial vehicles (UAV) have been increasingly used recently due to their high accessibility and technology growth. "Feature adaptation" is the process of finding similarities between two or more images from one scene obtained in different time intervals, viewing angles through various sensors. Application of this process in combination of obtained images and previous images can play a vital role in missions of UAV. In general, registration of two different images means finding common spots of two images considering occurred changes. It is obvious that images adaptation is one of applications of registration. All of images registration algorithms are done within 4 fundamental steps: identification and extraction of features, features adaptation, estimation of image transfer (or change) and conversion (or change in sampling rate) model. There are some constraints in each of steps that most of them are related to feature adaptation and extraction step. "Gaussian Mixture Model" has been recently employed for adaptation due to its simplicity and strength. Hence, this project has been conducted based on Gaussian model to improve quality and registration model in noisy environments toward rotation or resize.

Keywords: image registration, Gaussian Mixture Model, clustering, extraction of hotspots

1- Introduction

Unmanned aerial vehicles (UAV) have been increasingly used recently due to their high accessibility and technology growth. It is possible to collect information that is more effective from different areas using lightweight with high-resolution video cameras [1]. "Image adaptation" is a process of finding similarities between two or more images from one scene obtained in different time intervals, viewing angles through various sensors. Application of this process in combination of obtained images and previous images can play a vital role in missions of UAV [2, 3].

One another application of images registration is proper analysis of view including buildings, roads, etc. There are various problems in this field, because images will be resized in accordance with the distance between air camera and object. Moreover, roads might rotate without similar origin and distance of them to images.

In case of feature extraction, areas are first extracted from images in order to be strength to various changes including displacement, rotation, resize, change in brightness intensity, change in distance to camera, imagery, and image elongation [5].

2- Problem Statement

"Image adaptation" is a process of finding similarity between two or more images of one view in different time intervals and different viewing angles through different sensors. In case of geometric adaptation, two images (reference image and received image) are matched with each other to determine similar spots [7]. The initial technics of image adaptation required manual selection of control and prominent spots of images then these control spots were applied to estimate a conversion model in which, an image was matched with another image. Manual selection of each specific control spot is difficult and time-consuming, in particular in cases with large volume of information. Therefore, it is required to have automatic adaptation methods. Changed conditions in images acquisition including

fours factors of sensor type, time, location and imaged area nature lead to considerable differences between images so that these conditions might create problem in image adaptation process within one or several following forms [7, 8, 9].

1- Radiometric error: errors related to brightness level of pixels are referred to radiometric errors and errors created by information registration equipment.

2- Geometric errors: resources of geometric turbulences of earth rotation and panoramic effects (landscape change), non-ideal position of sensors, earth curvature and uncontrollable changes in position, height and angle of platform view.

3- Tissue problems: such as surfaces without tissue or weak tissue such as sea and farms, surfaces with repetitive tissues such as similar buildings, ambiguous surfaces such as the upside of tree and the land under it.

4- Change in views: such as changes occurred through passage of time such as seasonal changes and different farms cultivation in different seasons and other driving factors such as vehicles in large-scale images.

Hence, the objective of this research is to design an algorithm this is resistant to following parameters [5, 7]:

1- Strength: difference between various images obtained from one view exists because of some factors such as environmental noise, brightness difference, contrast and difference in viewing angle. Therefore, minimization of effect of such differences on accuracy of image adaptation is an important spot.

2- Efficiency: extraction of a proper number of correct correspondences in a low computational complexity indicates high efficiency of image adaptation algorithm.

3- Accuracy: imagination and analysis of information requires an acceptable level of accuracy in adaptation process.

4- Distinction: this factor indicates distinction between features and their descriptors compared to each other. Informational content is a criterion of distinction level of each feature.

In this research, two famous models of clustering [10] and probability distribution model (mixture Gaussian) [4] are studied.

In first model, clustering consists of feature vectors through an inter-collection structure. Cluster is a collection of similar data [10, 11].

In summary, the difference between clustering and classification is that each data in classification is allocated to a predetermined class but there is not any information about classes existed in data within clustering [12]. Finally, adaptation of features means finding the most similar features through clustering algorithm (such as k-means [13]).

In second model, an initial distribution of all features is considered. For instance, it is assumed that base probability distribution of all feature vectors is expressed by several means and variances [15]. Each feature vector in new images that was close to mean of each of distributions (through comparing of mean with variance) is matched with related distribution vectors [15, 16] then at next step, Euclidean distance between feature vectors related to distribution is examined based on new feature to match features accurately.

3- Theoretical Literature

Automotive registration methods have been developed over recent years [1, 3]. In this regard, specialized methods have been presented to register aerial images at high altitude in which, block can be seen partially [4, 6]. However, image registration at low altitude is one of considerable challenges in which, block issue can be seen [30].

Image registration has been used for target tracking over the years [7]. This subject led to problem solving in field of objective displacement or image transfer. On the other hand, overall displacement of consecutive frames or frame registration by mutual correlation has been determined. For instance, Jackowitz et al. [8] have applied phase correlation to register aerial images acquired from high altitude. Moreover, the moving objectives have been determined using this method and is traceable using related statistical models. Ayala et al. [10] divided each video frame to equal segments and traced segments frame by frame. Hence, the segment that was in contrary to the movement of its surrounding environment was excluded from trace. Jackson et al. [11] registered frames of a video range using a solid homographic matrix. This implementation method is similar to a video film in which, total surface of earth is modeled by an airplane throughout the view. In proposed method, earth surface can be changed throughout the view in terms of slope and height. The only condition for this method is flatness of earth at small local areas.

Then, hierarchy method was developed to register multiple images in accordance with expanded needs of proper aerial images registration [30].

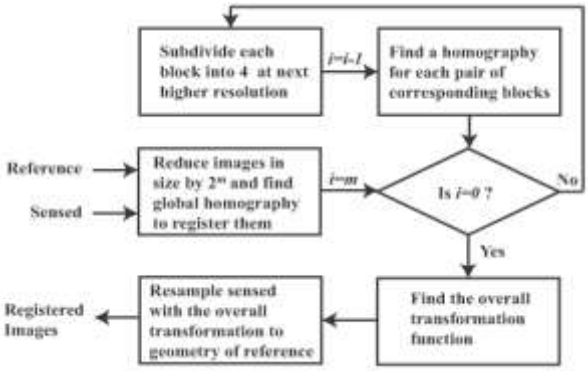


Figure 1. Hierarchical trend of image registration

When relevant signs are determined at highest resolution of images, a transfer function is used for overall surface and then various transfer functions are applied for image registration [16, 17].

To register images from different view spots of a 3-D view, a hybrid local and global homography was employed. Global homography are considered for different viewing angel between images captured by cameras and independent images of view content.

Local homography of view is dependent on local geometric differences between images captured in different view angles. Experiment of multiple aerial images of urban and suburban scenes with size of 30cm/pix indicates that block of 128×128 pixel consists of adequate signs to estimate homographic parameters and register blocks related to images. Therefore, if D is diameter of reference image, images should be reduced in size and factor 2^m is used for realization of following equation:

$$128 \leq \frac{D}{2^m} < 256. \quad (1\text{-}2)$$

If (x,y) and (X,Y) indicates coordinate of a view spot in reference and images with lowest resolutions, global homography can be written to register images with lowest resolution.

$$X = \frac{ax + by + c}{gx + hy + 1} \quad (1)$$

$$Y = \frac{dx + ey + f}{gx + hy + 1} \quad (2)$$

If images are considered at scale with observation coefficient to obtain new images with coordinate of (x',y'), (X',Y'),

$$x' = sx \quad y' = sy \quad X' = sX \quad Y' = sY \quad (3)$$

then, componnets of x, y, X, Y are written based on x',y', X',Y' and replaced with two above equations to obtain relations between (x,y) and (X,Y)

$$X' = \frac{ax' + by' + cs}{\left(\frac{g}{s}\right)x' + \left(\frac{h}{s}\right)y' + 1} \quad (4)$$

$$Y' = \frac{dx' + ey' + fs}{\left(\frac{g}{s}\right)x' + \left(\frac{h}{s}\right)y' + 1}. \quad (5)$$

Equations (4) and (5) indicate that global homography is once calculated for images. Hence, it can be applied to register these small images with scale s replacing c with cs, f with fs, g with g/s and h with h/s. Therefore, global homography is found by a-h parameters to register images at lowest resolution and similar images at highest resolution

can be obtained at global level (although approximately) by scaling registration of homographic parameters (equations (4) and (5)).

Equations (1) and (2) consist of 8 passive parameters that require four or more relevant signs in images. It is required to determine four relevant signs in images through a completely automatic method. The relevant turning spot can be obtained within two steps. First, a collection of signs is determined in each image then corresponds between two collections of spots can be seen.

Local sign are unique in images. These signs in images would facilitate search for relevant area. Numerous turning spot's detection methods have been developed over recent years [18, 19]. Two Heris [20] and screening [21] detectors are extensively employed. The first one extracts hotspots based on corners and second one identifies important areas.

In this chapter, concentration is on images from urban and suburban views using Heris detector as presumption and SIFT detector as substituent.

SIFT detector describes various features in the neighborhood of a turning spot. Hence, 128 features including gradient features description of neighborhood intensity of a turning spot is used in this vector detector algorithm. If Heris corner detector is employed, relevant features should be calculated for each corner. To reach the highest speed herein, radius 12 is determined experimentally; whereas, obtaining adequate geometric local information is doable in case of centralized pattern at turning spot when working with 30cm/pix images.

To reduce geometric difference locally between images, this global homography is determined once so that images can be registered at global level using homography. This resolution of images can be gradually increased and the obtained correspond in resolution is used to redefinition of transformations of a low-level resolution and then corresponds considered between signs in images are determined using following rules.

1- For each turning spot in reference image, turning spot is found in second image. This spot is identifiable calculating the nearest vector calculation (measuring Euclidean distance).

2- If turning spot is ended in second image in order to be corresponded with more than one turning spot in reference image, all ambiguous correspond spots are removed.

3- Residual corresponds which are unique are considered correspond spots.

Images usually consist of blocked areas along with depth discontinuity from different 3-D views. Since the location of discontinuities' depth is not pre-identified, it is a significant challenge to identify hotspots in blocked areas. In this case, the results of RANSAC algorithm will be matched with error. Homogeneous blocks do not generate any sign; hence, there will not be any adaptation result.

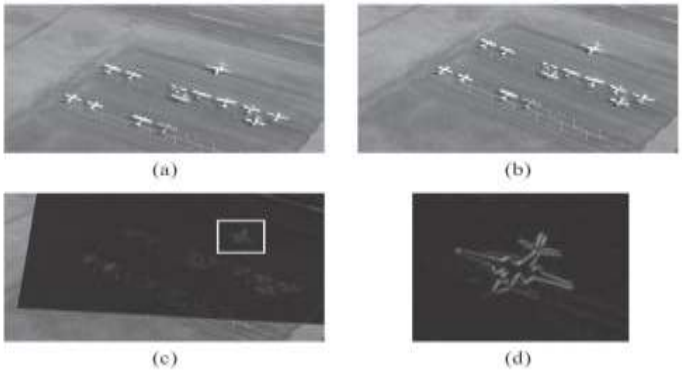


Figure 2. (a) and (b) Aerial images from airport with homogenous and blocked areas

These images are 720×1280 in size. (c) is absolute amount of intensity difference of registered images at earth surface with matrixes composition. (d) is a close schema of difference image in a window of airplane.

Consider images of airplane indicated in figure 2 (a) and (b). Generated signs in images show airplane corner on the earth. Paved and green areas hardly generate signs. Low-resolution images are hardly signed using registered signs by airplane and signing on the earth so that both estimated models indicate limited homography. The result obtained from registration has error hardly determined using overall homographic matrix. Therefore, non-registered objects seem above the earth surface and it is because of different image caused by depiction of difference corner between images that is illustrated in parts (c) and (d) of the figure 2. Database consists of 17 aerial videos captured by a helicopter throughout the province that its surrounding area is like a circular route at the same height to generate a route with 30cm/pix in length at earth surface. One frame of each video has been illustrated in figure 3. White-black videos are

available expect for 13 images that are only depicted at gray scale. A detector that works with color information [30] is employed at the time of frame registration in a colored video to identify important locations.

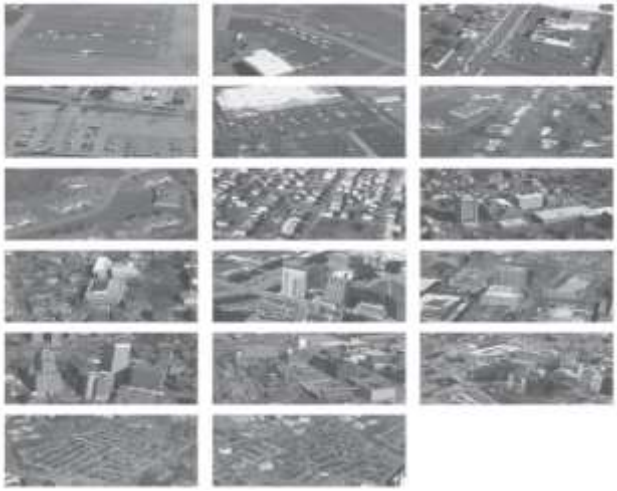


Figure 3. A frame of each 17 videos used at this study

These videos indicate some flat areas and tall buildings. If videos consists of N frames, frame I is registered as i+k frame skipping from k-1 frame. Frame 0 is registered as frame k and frame 1 is registered as frame k+1 and as the same way frame N-k-1 is registered as N-1. For a video consisting of frame N and k-1 frame skipping (K≥1), there will be N-k-1 frames for registration at the time of frame registration.

Table 1. Independence of proposed model to view content and difference of viewing angle between consecutive frames

Video	1	2	3	4	5	6	7	8	9
N	194	192	312	185	219	222	239	407	336
k	3	3	3	6	4	5	4	3	3
Video	10	11	12	13	14	15	16	17	
N	336	349	364	180	112	102	387	354	
k	2	2	2	2	1	1	6	3	

N frames are indicated in a video at second row and difference of maximum frame number in a video is indicated at third row without breaking chain consolidation.

No frame is removed foe each video at the time of frame registration (k=1). If all frames have successful trends, k+1 registration will have and this trend will repeat until one pair of frame is registered consecutively. This trend will be registered if images at high levels (low resolutions) exist; therefore, images at lower levels might not be registered. When two frames are registered in correct sequence, average absolute amount of intensity difference between relevant signs is small, but when two frames are not correctly registered, this brightness intensity difference is relatively large. In our project, when average of absolute intensity difference is increased in correspond signs in registration, it is controlled by a factor more than twice replications compared with prior registration. Some other actions are proposed to prevent from inaccurate registration [30].

The results obtained from 17 videos are indicated in table 1. Successive frame of a video consisting of tall buildings have more blocks and Euclidean differences of successive frames in one video are relative major. For instance, increase speed of cameral movement would increase difference of viewing angle between successive frames. Since difference of viewing angle is major and building is taller, the block is increased and Euclidean difference between successive frames will expand.

Frames 100 and 102 of video 13 are considered to show this phenomenon. These images are depicted in figure 6 (a) and (b). Absolute amount of brightness intensity of images after registration are illustrated in (c) and (d).

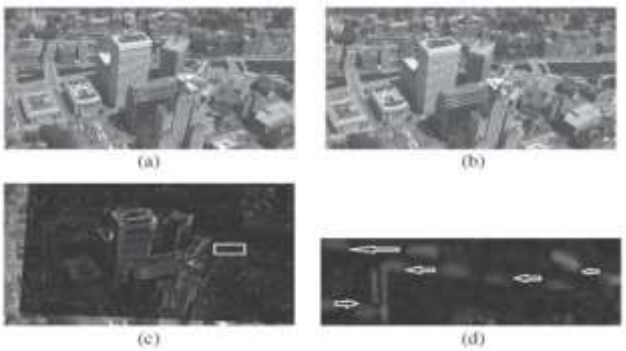


Figure 4. (a) and (b) are frames 100 and 102 of video 13; (c) is frame registration on earth surface using hybrid method and area inside of window is enlarged in (d) for better observation

Moving vehicle seems like a clear bubble. The motion arrow of automobile from frame 100 to frame 102 is indicated. A small area of figure 4 (c) is magnified that is indicated in figure 4(d) for better observation.
Automobile movement from frame 100 to frame 105 is shown by an arrow. Earth surface seems dark after registration. Moving car seems like a clear bubble contrary to dark earth. Finally, images of a coastal city are shown in (e) and (d) parts of figure 5 as well as homogenous areas for registration evaluation.

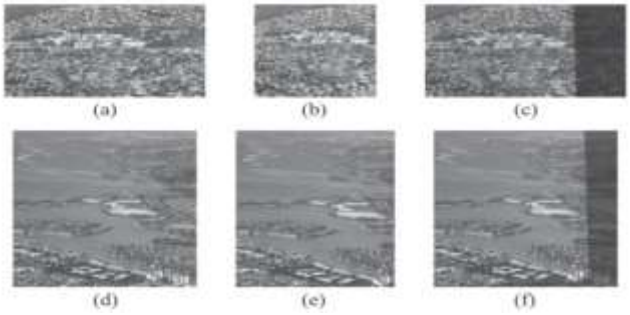


Figure 5. (a) and (b) are images of different views of a landscape full of urban hills, (c) is images registrations, (d) and (e) are images from a coastal city with considerable homogenous areas and presence of waves irregular movement from one image to another

Sizes of image (a), (b), (d), and (e) are equal to 877×1510, 1076×1130, 2271×1844, and 2292×2155, respectively that are registered using hybrid method.
Assuming that {M,S} are a collection of two spots with limited size for registration, this collection of aerial image are extracted using feature detector. In this case, M is the model of label regulation movement and S is related to constant scene. All of two M and S collections are assumed as sub-collections of a definite vector of a real space of R^d.
According to the algorithm of strong spot collection, a discrete spot collection is indicated by continuous density function so that probability density function from a general mixture Gaussian is defined as follows:

$$p(x) = \sum_{i=1}^{k} w_i \varphi\left(x|\mu_i, \sum_i\right) \quad (1\text{-}3)$$

$$\varphi\left(x|\mu_i, \sum_i\right) = \frac{\exp\left[-\frac{1}{2}(x-\mu_i)^T \sum_i^{-1}(x-\mu_i)\right]}{\sqrt{(2\pi)^d |\det(\sum_i)|}}$$

If segments numbers are enough large, any density can be properly described by this approximate model: 1) a number of Gaussian components are regulated with number of spots around each spot and all components are equal in weight;

2) for each component, location position vector of each spot is given; 3) all segments have shared spherical covariance matrix that is an estimation of image parameters.
Then L_2 distance between two mixture Gaussians are calculated. In particular, the purpose of this study is to calculate parameter θ (parameter independent to place transfer matrix of T) in accordance with collection of model M and collection of scene S for transformation group that minimizes following cost functions:

$$d_{L_2}(S,M,\theta) = \int (gmm(S) - gmm(T(M,\theta)))^2 \, dx \quad (6)$$

Where, gmm (p) indicates density of mixture Gaussian created by considered spot. Therefore, gradient calculation method can be applied to optimize cost functions. According to stringent transformation model, moving model around spot M and collection of main spot of model M_0; hence, we tend to find proper movement equation of $M=M_0R^T+t$ in which, R is rotation matrix and t is transfer vector. Let I_n next column vector obtained from all derivatives of cost function in accordance with movement of parameters t and R.

$$\begin{cases} \dfrac{\partial F}{\partial t} = G^T 1_m \\ \dfrac{\partial F}{\partial r_i} = 1_d^T \left((G^T M_0) \otimes \left(\dfrac{\partial R}{\partial r_i} \right) \right) 1_d \end{cases} \quad (7)$$

Where, $(r_1 \ldots r_i)$ are parameters of rotation matrix R and $\otimes$ is Germanic multiplication. A legal term should be optimized at the time of costs functions optimization using a numerical search engine. However, it is difficult to find a direct solution in accordance with different size of images. In this part, a collection of parametric borders is the same images size. This model is changed when size of model image and scene image is changed without effecting on accuracy of algorithm, but adding algorithm contributes to more algorithm improvement.
Contour adaptation of images is simply done comparing histogram diagrams. First, each contour should change to vector codes $\{c_i\}_j$ that indicates jth contour:

$$c_i = \begin{cases} \arccos(\Delta x_i, \Delta y_i), & \Delta y_i \le 0 \\ \arccos(-\Delta x_i, -\Delta y_i), & \Delta y_i > 0 \end{cases} \quad (8)$$

Where, $(\Delta x_i, \Delta y_i) = P_{i+1} - P_i$, P_i is defined as ith spot in contour. Therefore, each contour is related to one histogram. Hence, contour adaptation is considered as a histogram adaptation problem. Metric similarity is defined as follows:

$$d(H_1, H_2) = \sqrt{1 - \sum_i \frac{\sqrt{H_1(i)H_2(i)}}{\sqrt{\sum_i H_1(i) \sum_i H_2(i)}}} \quad (9)$$

Where, H is calculated histogram from chain codes.

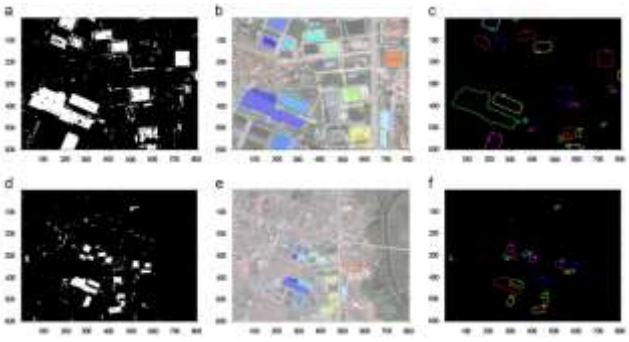


Figure 6. Feature detector performance

The first row indicates the result of image captured from 1km distance. The second row indicates image captured from 3km distance.
In first experiment, images are completely aligned and then the proper feature detector is selected then important areas in main images can be identified.
Second experiment indicates performance of proposed image registration method based on mixture Gaussian model. To indicate performance of proposed algorithm, four pairs of spots as data collection extracted from images is considered as following figure (a).

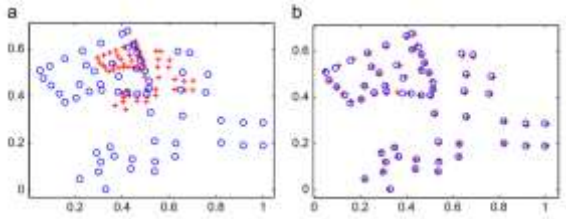


Figure 7. Image registration method based on mixture Gaussian model

Spots "+" are selected in 3km and 1km, respectively. (a) is initial spot of collections and (b) is registration result.

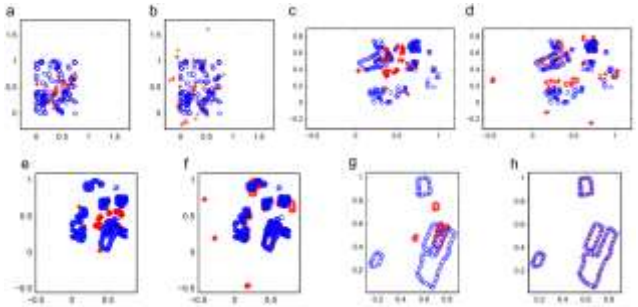


Figure 8. Comparing performance of different feature spot extraction for image registration

(a) and (b) indicate initial spot collection and registration results, respectively, using Harris-Laplace detector ; (c) and (d) indicate initial spot collection and registration results, respectively, using corner detector of canny; (e) and (c) indicate result of presented method without adaptation lines; and (g) and (h) indicate statistical method using a general registration step.
In third experiment, several spots are compered using different feature extraction methods and its performance evaluation within image registration. According to following figure (a) and (b), noisy spots are located in middle of image. If feature spots are expanded using a corner detector of canny, the obtained results indicated in figure (3-3) (c) and (d) will be obtained.

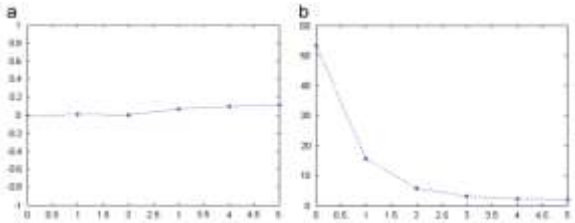


Figure 9. Relation between registration performance and re-sampling time; (a) is the relation between mean deviation and re-sampling time and (b) is the relation between implementation time and re-sampling time

The most important step to use proposed algorithm is providing suitable images. In this regard, two main types of graph including directed and undirected graphs can be used for modeling of a collection of spot data. In this research, the image is modeled in frame of undirected graph. Clustring algorithm of k-means will be stopped if objective function is minimized. Contrary to K-mean algorithm, clustering algorithm of FCM allows elements being belonged to more than one cluster. The following equation indicates minimization of objective function within FCM clustering.

(10)

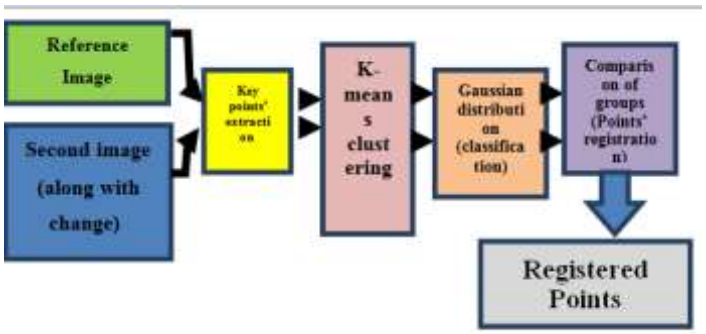


Figure 10. Diagram of proposed algorithm

The most important step is preparing suitable images. Images existed in Standard Data collection of ASD* (images in part B) [2] have been applied in present project.



Figure 11. Different aerial images of ASD [2]

As can be seen, aerial images are colored with a high quality suitable for adaptation and registration of images. Also, there are considered subjects with different sizes in this database so that their location angles are differently observed through camera lens.

* http://web.ornl.gov/~jiy/ASD/Aerial%20Image%20Segmentation%20Dataset.html



Figure 12. Extraction of key spots for registration

At second step, spots are classified by K-means algorithm so that similar spots are categorized in a same class.



Figure 13. Results obtained from spots clustering through proposed algorithm

At third step, each group is expressed by a Gaussian distribution and then Gaussian distribution obtained from two reference and test images are compared with each other.

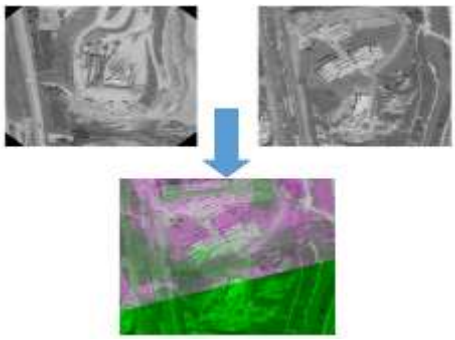


Figure 14. Observational results obtained from registration of two first images by database

Purple spots are registered spots and green spots are non-registered spots. Hence, most of the spots of second image have been registered compared to first image.

Algorithm	**First image pair**	**Second image pair**
proposed	70%	83%
probable registration [2]	65%	80%

According to table, the closer the registration amount is to 1 or 100%, the more registered spots will have. Hence, it can be seen through comparing amounts that registration accuracy in proposed algorithm is better than registration

accuracy in similar approaches. Accordingly, it is expected that more accurate amounts with less computational errors developing the mentioned approach.

4- Results

The main process of this project was based on three steps including 1- extraction of key spots from input images, 2- data clustering using k-means algorithm, 3- description of each group using Gaussian distribution. Finally, similarities between spots are calculated and images are registered comparing distributions and finding Euclidean distances between them. Relevant images are extracted from ASD database and exploited. Adaptation accuracy results obtained from this database considering various parameters indicated high accuracy of the used approach through finding similar spots despite rotation and scale changes, because considered spots can be adapted and registered properly using Gaussian probability model and data clustering.

References

[1] J. Thirion and G. Calmon, "Deformation analysis to detect and quantify active lesions in three-dimensional medical image sequences," IEEE Trans. Med. Imag. , vol. 18, no. 5, pp. 429–441, May 1999.
[2] W. Chuan, W. Yuanyuan, H. R. Karimi, "A robust aerial image registration method using Gaussian mixture models", Elsevier Journal of NeuroComputing, 2014.
[3] M. Bosc, F. Heitz, J. Armspach, I. Namer, D. Gounot, and L. Rumbach, "Automatic change detection in multimodal serial MRI: Application to multiple sclerosis lesion evolution," Neuroimage, vol. 20, no. 2, pp. 643–656, 2003.
[4] Q. Liu, R. J. Sclabassi, and M. Sun, "A new change detection method and its application to epilepsy monitoring video," inProc. IEEE 30th Annu. Northeast Bioeng. Conf. , Apr. 2004, pp. 59–60.
[5] J. Collins and C. Woodcock, "An assessment of several linear change detection techniques for mapping forest mortality using multitemporal Landsat TM data,"Remote Sensing Environ. , vol. 56, no. 1, pp. 66–77, 1996.
[6] H. Gonçalves, L. Corte-Real, and J. A. Gonçalves, "Automatic image registration through image segmentation and SIFT," IEEE Trans. Geosci. Remote Sens., vol. 49, no. 7, pp. 2589–2600, Jul. 2011.
[7] T. Kim and Y.-J. Im, "Automatic satellite image registration by combination of matching and random sample consensus," IEEE Trans. Geosci. Remote Sens., vol. 41, no. 5, pp. 1111–1117, May 2011.
[8] A. Wong and D. A. Clausi, "ARRSI: Automatic registration of remotesensing images," IEEE Trans. Geosci. Remote Sens., vol. 45, no. 5, pp. 1483–1493, May 2007.
[9] X. Fan, H. Rhody, and E. Saber, "A spatial-feature-enhanced MMI algorithm for multimodal airborne image registration," IEEE Trans. Geosci. Remote Sens., vol. 48, no. 6, pp. 2580–2589, Jun. 2010.
[10] Z. Liu, J. An, and Y. Jing, "A simple and robust feature spot matching algorithm based on restricted spatial order constraints for aerial image registration," IEEE Trans. Geosci. Remote Sens., vol. 50, no. 2, pp. 514–527, Feb. 2012.
[11] J. Ma, J. C.-W. Chan, and F. Canters, "Fully automatic subpixel image registration of multiangle CHRIS/Proba data," IEEE Trans. Geosci. Remote Sens., vol. 48, no. 7, pp. 2829–2839, Jul. 2010.
[12] P. Cheng and C.-H. Menq, "Real-time continuous image registration enabling ultraprecise 2-D motion tracking," IEEE Trans. Image Process., vol. 22, no. 5, pp. 2081–2090, May 2013.
[13] K. Jackovitz, V. Asari, E. Balster, J. Vasquez, and P. Hytla, "Registration of region of interest for object tracking applications in wide area motion imagery," in Proc. AIPR, 2012, pp. 1–8.
[14] X. Mei and F. Porikli, "Joint tracking and video registration by factorial hidden Markov models," in Proc. IEEE Int. Conf. Acoust., Speech Signal Process., 2008, pp. 973–976.
[15] I. L. Ayala, D. A. Orton, J. B. Larson, and D. F. Elliott, "Moving target tracking using symbolic registration," IEEE Trans. Pattern Anal. Mach. Intell., vol. 4, no. 5, pp. 515–520, Sep. 1982.
[16] B. P. Jackson and A. A. Goshtasby, "Registering aerial video images using the projective constraint," IEEE Trans. Image Process., vol. 19, no. 3, pp. 795–804, Mar. 2010.
[17] M. Gong, S. Zhao, L. Jiao, D. Tian, and S. Wang, "A novel coarse-to-fine scheme for automatic image registration based on SIFT and mutual information," IEEE Trans. Geosci. Remote Sens., vol. 52, no. 7, pp. 4328–4338, Jul. 2014.
[18] B. P. Jackson and A. A. Goshtasby, "Adaptive registration of very large images," in Proc. CVPR Workshop Registration Very Large Images, Columbus, OH, Canada, Jun. 2014, pp. 345–350.
[19] S. R. Lee, "A coarse-to-fine approach for remote-sensing image registration based on a local method," Int. J. Smart Sens. Intell. Syst., vol. 3, no. 4, pp. 690–702, Dec. 2010.
[20] B. Likar and F. Pernus, "A hierarchical approach to elastic registration based on mutual information," Image Vis. Comput., vol. 19, no. 1/2, pp. 33–44, Jan. 2001.
[21] A. Goshtasby, "Registration of images with geometric distortions," IEEE Trans. Geosci. Remote Sens., vol. 26, no. 1, pp. 60–64, Jan. 1988.

[22] F. L. Bookstein, “Principal warps: Thin-plate splines and the decomposition of deformations,” IEEE Trans. Pattern Anal. Mach. Intell., vol. 11, no. 6, pp. 567–585, Jun. 1989.
[23] S. Gauglitz, T. Höllerer, and M. Turk, “Evaluation of interest spot detectors and feature descriptors for visual tracking,” Int. J. Comput. Vis., vol. 94, no. 3, pp. 335–360, Sep. 2011.
[24] T. Tyutelaars and K. Mikolajczyk, “Local invariant feature detectors: A survey,” Found. Trends Comput. Graph. Vis., vol. 3, no. 3, pp. 177–280, Jan. 2008.
[25] C. Harris and M. Stephens, “A combined corner and edge detector,” in Proc. 4th AVC, 1988, pp. 147–151.
[26] D. Lowe, “Distinctive image features from scale-invariant keyspots,” Int. J. Comput. Vis., vol. 60, no. 2, pp. 91–110, Nov. 2004.
[27] A. Goshtasby, Image Registration: Principles, Tools and Methods. New York, NY, USA: Springer-Verlag, 2012.
[28] R. Hartley and A. Zisserman, Multiple View Geometry in Computer Vision, 2nd ed. Cambridge, U.K.: Cambridge Univ. Press, 2003, ch. 4.
[29] P. Chen and D. Suter, “Rank constraints for homographies over two views: Revisiting the rank four constraint,” Int. J. Comput. Vis., vol. 81, no. 2, pp. 205–225, Feb. 2009.
[30] M. E. Linger, A. A. Goshtasby, "Aerial Image Registration for Tracking," IEEE Transactions in Geoscience and Remote Sensing, vol. 53, no. 4, pp.2137-2145, April 2015.
[31] D. Shepard, “A two-dimensional interpolation function for irregularly spaced data,” in Proc. 23rd Nat. Conf. ACM, 1968, pp. 517–524.
[32] E. Molina and Z. Zhu, “Persistent aerial video registration and fast multi-view